SCIENTIFIC REPORTS

OPEN

SUBJECT AREAS:
STRUCTURAL PROPERTIES
NANOSCALE MATERIALS

Received
4 November 2014

Accepted
31 December 2014

Published
28 January 2015

Correspondence and requests for materials should be addressed to F.S.-S.C. (fsschien@thu.edu.tw)

Revealing the flexoelectricity in the mixed-phase regions of epitaxial $BiFeO_3$ thin films

Cheng-En Cheng[1,2], Heng-Jui Liu[3], Franco Dinelli[4], Yi-Chun Chen[5], Chen-Shiung Chang[1], Forest Shih-Sen Chien[2] & Ying-Hao Chu[3]

[1]Department of Photonics and Institute of Electro-Optical Engineering, National Chiao Tung University, Hsinchu, 30010, Taiwan, [2]Department of Applied Physics, Tunghai University, Taichung, 40704, Taiwan, [3]Department of Materials Science and Engineering, National Chiao Tung University, Hsinchu, 30010, Taiwan, [4]Consiglio Nazionale delle Ricerche, Istituto Nazionale di Ottica, I-56124 Pisa, Italy, [5]Department of Physics, National Cheng Kung University, Tainan, 701, Taiwan.

Understanding the elastic response on the nanoscale phase boundaries of multiferroics is an essential issue in order to explain their exotic behaviour. Mixed-phase $BiFeO_3$ films, epitaxially grown on $LaAlO_3$ (001) substrates, have been investigated by means of scanning probe microscopy to characterize the elastic and piezoelectric responses in the mixed-phase region of rhombohedral-like monoclinic (M_I) and tilted tetragonal-like monoclinic ($M_{II,tilt}$) phases. Ultrasonic force microscopy reveal that the regions with low/high stiffness values topologically coincide with the $M_I/M_{II,tilt}$ phases. X-ray diffraction strain analysis confirms that the M_I phase is more compliant than the $M_{II,tilt}$ one. Significantly, the correlation between elastic modulation and piezoresponse across the mixed-phase regions manifests that the flexoelectric effect results in the enhancement of the piezoresponse at the phase boundaries and in the M_I regions. This accounts for the giant electromechanical effect in strained mixed-phase $BiFeO_3$ films.

In the race for the development of sensing and actuation applications, a lot of attention has been paid to the search for materials with large mechanical response via external stimuli, such as piezoelectrics and shape memory alloys[1]. These materials present a complexity of phase constitutions, and the transformation between different phases plays a crucial role in showing large electromechanical responses[2]. Perovskite $BiFeO_3$ (BFO) is found to be a green piezo/ferroelectric material with longitudinal piezoelectric coefficient[3] (d_{33}) larger than 60 pm/V and spontaneous ferroelectric polarization[4] of about 100 $\mu C/cm^2$. Therefore, BFO has been considered as a good candidate to replace current Pb-based piezoelectrics.

Via imposing epitaxial strain to BFO films, the ground phase can be tuned from rhombohedral (R) to tetragonal (T) or orthorhombic, depending on the degree of strain and its sign (compressive or tensile)[5–7]. Furthermore, by employing suitable substrates and thickness values, the R-like monoclinic M_I and T-like monoclinic M_{II} phases can coexist to form nanoscale self-organized alternative stripes[8]. These self-organized phase boundaries provide a superior template to understand the fundamental physics underlying the giant electromechanical responses. Recently, researchers have thus spent a lot of efforts making relevant progresses. Some studies, carried out with techniques such as atomic force microscopy (AFM), X-ray diffraction (XRD), and transmission electron microscopy (TEM), suggest that the giant piezoelectric response in mixed-phase BFO films can be attributed to a phase transformation from M_{II} to mixed M_I-M_{II}[8–10]. The phase boundaries in mixed-phase BFO films show an extraordinary enhancement of their piezoelectric response, e.g., a remarkably high d_{33} ($\sim$ 400 pm/V)[11]. Such a superior piezoelectric response can be possibly associated with the flexoelectric effect. In addition to its superior piezoelectric response, intriguing magnetism properties have been also found[12]. Their origins can be attributed to either piezomagnetic or flexomagnetic effects[11]. The flexoelectric effect is the polarization response of materials to a strain gradient ($\partial u/\partial x$), i.e., an inhomogeneous deformation due to a break in centro-symmetry. The bulk electromechanical polarization (P) can be described with the following equation:

$$P = \chi E + \mu \frac{\partial u}{\partial x}. \quad (1)$$

On the right hand side of Eq. (1), the first term is the dielectric response with the dielectric susceptibility χ, and the second term is the flexoelectric response with the flexoelectric coefficient μ. Flexoelectricity is of great interest for the development of nanoscale technologies, because large strain variations often present on the nanoscale to produce a strong flexoelectric effect[13].

Most of these studies are based on structural or electrical and magnetic properties. However it is also very important to understand the elastic modulation of these phase boundaries, which could help to individuate the direct causes for large flexoelectricity in BFO. Studying the elastic moduli of nanometric mixed-phase regions in sub-100 nm-thick BFO films is a severe challenge for conventional techniques (such as Nanoindentation), because they do not provide sufficient spatial resolution. AFM possesses the required resolution to characterize local elastic properties of compliant materials such as polymers. However, the cantilevers employed in AFM are relatively too compliant (typically the spring constant is well under 100 N/m) to distinguish the elastic difference of very stiff materials, e.g., semiconductors and metal oxides. Ultrasonic force microscopy (UFM) is an offspring of AFM specifically developed to measure the local elastic properties of stiff materials with compliant cantilevers[14–16]. UFM operates by detecting the intrinsic nonlinearity of the probe-sample interaction, thanks to the application of a vertical vibration to the sample at an ultrasonic frequency (i.e., the exciting frequency is much higher than the fundamental resonant frequency of the cantilever and off higher resonances).

In this paper, the topography, stiffness and piezoresponse of mixed-phase BFO are investigated by scanning probe techniques, i.e., AFM, UFM and piezoresponse force microscopy (PFM). It is demonstrated that UFM can qualitatively investigate the elastic modulation inside the mixed-phase regions of BFO thin films. Unlike the stiffer pure R-phase BFO, the stiffness of the R-like M_I phase is found to be lower than that of the T-like M_{II} phase. XRD strain analysis by means of reciprocal space mapping (RSM) has been also carried out. The RSM results are in good agreement with the UFM findings. The elastic modulus exhibits kinks at the phase boundaries and higher elastic gradient in the M_I phase. The correlation between the elastic modulation and piezoresponse in mixed-phase regions indicates that the flexoelectric effect causes the piezoresponse peaks at the phase boundaries and a higher piezoresponse inside the M_I regions compared to that inside the M_{II} and tilted T-like monoclinic $M_{II,tilt}$ regions.

Results

Scanning probe characterizations. The topography (AFM), the elastic response (UFM) and out-of-plane (OP) piezoresponse of the same area are shown in Fig. 1. Topography can be acquired simultaneously to either UFM or PFM images. In this case, we only report one AFM image, as they are identical. The topographic image shows the atomic flat terraces of M_{II} matrix and the mixed-phase regions. The mixed phase regions consist of the M_I and $M_{II,tilt}$ phases[12]. The M_I and $M_{II,tilt}$ phases can be considered as intermediate phases making it possible a continuous transition from the highly-strained M_{II} phase to the highly-relaxed distorted R phase with increasing film thickness. The UFM image shows a clear contrast in the mixed-phase regions (Fig. 1b), indicating that UFM can resolve the elastic properties of the stripes on the nanoscale. A well detectable elastic modulation is noticeable across these regions, i.e., the stiffness is not uniform. Curved loops of the OP-PFM image belong to the $M_I/M_{II,tilt}$ phase boundaries and each M_I phase region is enclosed by a loop (Fig. 1c)[12,17]. On the other hand, the elastic modulation well correlates with the topographic and piezoresponse features.

To better illustrate the correlations among topography, stiffness and piezoelectricity in the mixed-phase regions, the line profile at the mixed-phase regions of the AFM image and the corresponding

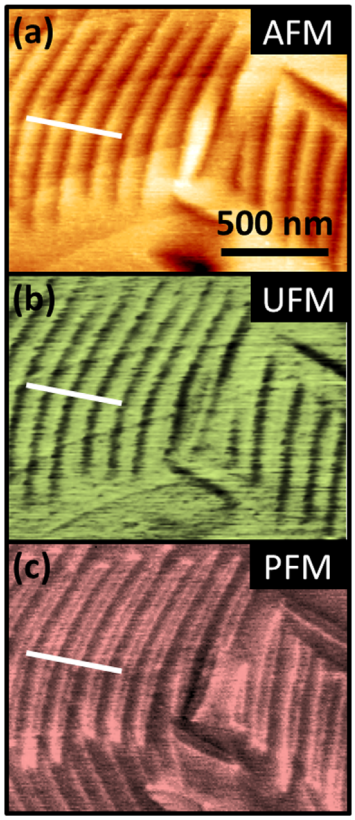

Figure 1 | AFM (a), UFM (b) and PFM (c) images of a 70 nm BFO film on LAO, giving a representative view of the surface in terms of topography, stiffness, and piezoresponse.

profiles of UFM and PFM are shown in Fig. 2. The mixed-phase regions exhibit an asymmetric peak-and-valley landscape (Fig. 2a), where the tilted angles of left and right sides of the peaks are 2.6° and 1.6°, respectively[8,12]. The left/right sides of a peak are the areas of the

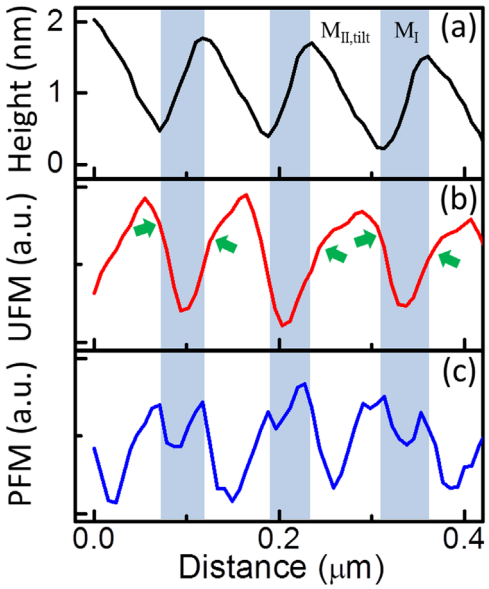

Figure 2 | Profiles of topography (a), stiffness (b) and piezoresponse (c) along the lines across the same mixed-phase regions drawn in Fig. 1. The shadowed areas indicate the M_I phase and the others the $M_{II,tilt}$ phase. The arrows in (b) indicate the kinks of the elastic modulation at the boundaries.

$M_I/M_{II,tilt}$ phases with widths of approximately 35 and 80 nm, respectively. These peaks and valleys are exactly the phase boundaries between the M_I and $M_{II,tilt}$ phases. From the stiffness profile (Fig. 2b), the low/high stiffness values topologically coincide with the $M_I/M_{II,tilt}$ phases, indicating that the M_I phase has an elastic modulus lower than that of $M_{II,tilt}$ phase.

Both experimental and theoretical studies demonstrate that the elastic modulus of the strain-free R phase (from 130 to 200 GPa, depending on the direction of interest) is higher than that of the highly-strain M_{II} phase (~100 GPa)[18–20]. Calculations by means of first-principles density-function theory (DFT) also confirm that BFO with a lower unit-cell volume has a higher elastic modulus. Based on the TEM results, the average lattice parameters of the M_I phase can be still estimated as $a = b \approx 3.82$ Å, $c \approx 4.16$ Å in a pseudo-tetragonal form, significantly different from that of the R phase ($a = b \approx 3.92$ Å, $c \approx 4.01$ Å). These observations indicate that the M_I phase has the smallest unit-cell volume (12.14 Å^3 per atom) compared to the other phases (13.28 Å^3 per atom for the M_{II} phase and 12.32 Å^3 per atom for the R phase). Thus, the M_I phase should be the toughest one according to this supposition. Nevertheless, the UFM data in terms of the stiffness in the mixed-phase regions are against the DFT prediction.

X-ray diffraction strain analysis. To verify the UFM findings, room-temperature RSM has been then performed. RSM data of the partially-relaxed BFO thin film on $LaAlO_3$ (001) substrate (LAO) include the diffraction peaks of the M_I, M_{II} and $M_{II,tilt}$ phases (Fig. 3). The M_I phase has a lattice constant in c axis of 4.16 Å, whereas M_{II} and $M_{II,tilt}$ phases have an identical lattice constant ($c = 4.65$ Å). Both the M_I and $M_{II,tilt}$ phases have an off-normal c-axis orientation, where the M_I phase has a tilted angle of 2.8° and the $M_{II,tilt}$ phase of 1.6°. The tilted angle values are well consistent with the results obtained from the AFM topography. Fig. 4 shows the diffraction profiles across the $M_{II,tilt}$ peaks in Q_x and Q_z, and the M_I peak in the longitudinal direction. The peaks can be fitted by Gaussian functions; the full widths at half maximum (FWHM) of those peaks are listed in Table I. The FWHM of the M_I peak in Q_x/Q_z is the x/z component of the FWHM in the longitudinal direction. Obviously, the peak of the M_I phase is wider than that of the $M_{II,tilt}$ phase by 58% in Q_x and 33% in Q_z. The wider peak in the Q_x reflects the misorientation of the c axis, while the wider peak in the Q_z reflects a larger distortion in the c-axis spacing and/or a smaller grain size in the c axis. From the cross-section TEM image, reported in the supplementary materials by Liu *et al.*[8], the M_I and $M_{II,tilt}$ phases have a well epitaxial relationship with the M_{II} phase and the substrate. The grains of all phases extend from the surface to the substrate, so those phases have the same grain size along the out-of-plane direction. Therefore, the broadness in Q_z of M_I phase is merely attributed to the distortion of the c-axis spacing instead of a grain size

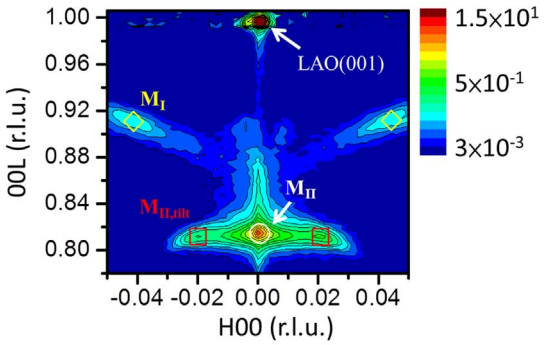

Figure 3 | RSM of BFO thin films around the direction LAO (001) in order to show the diffraction peaks of the R, M_I (diamond), M_{II} (circle) and $M_{II,tilt}$ (square) phases.

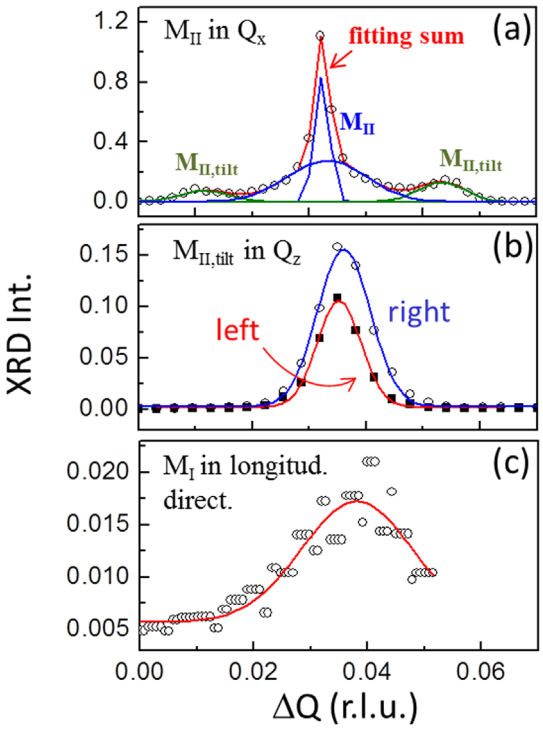

Figure 4 | XRD Peak profiles of (a) the M_{II} (blue) and $M_{II,tilt}$ (olive) phases in Q_x, (b) the $M_{II,tilt}$ phase in Q_z, and (c) the M_I phase in the longitudinal direction. The peak of the M_{II} phase can be deconvoluted into two components of crystalline and diffusive scatterings due to the fact that the film thickness is of only 70 nm.

effect. The larger misorientation and spacing distortion of the c-axis of the M_I phase depict its more ambiguous lattice structure, which implies that the stiffness in the M_I phase is lower than that in $M_{II,tilt}$.

Furthermore, the lower value in stiffness of the M_I phase can be evidenced from the structural aspect. In the mixed region, the M_I and $M_{II,tilt}$ phases are the products of the strain relaxation and the intermediate phases to connect with the M_{II} and R phases. The $M_{II,tilt}$ phase has the same structure of the M_{II} phase but slightly tilted with respect to the surface normal. The M_I phase has a large tilted angle and the smallest lattice structure. For compensating the difference of height between the M_{II} and R phases, M_I varies more dramatically (a transverse distance of about 35 nm with a tilted angle of 2.8° on the macroscale) than $M_{II,tilt}$ (a transverse distance of about 80 nm with a tilted angle of 1.6° on the macroscale), implying that M_I is softer than $M_{II,tilt}$. Therefore, we suggest that the intermediate M_I phase is not in the low energy state, and not so rigid and stable as the R and M_{II} phases, thus being more compliant than the other phases.

Flexoelectric effect. The correlation between the stiffness and piezoresponse profiles (Fig. 2b and 2c) can illustrate the flexoelectric effect in mixed-phase BFO films. From the stiffness profile, Kinks at the interface indicate a strain discontinuity between M_I and $M_{II,tilt}$ phases. Those kinks coincide with the piezoelectric peaks at the boundaries, which implies that the flexoelectric effect results in the enhancement of piezoresponse. In addition, the slope of stiffness on the M_I side is higher than that on the $M_{II,tilt}$ side, indicating that the elastic (strain) gradient in the M_I phase is higher than that in the $M_{II,tilt}$ phase. Besides the piezoresponse inside the more compliant M_I regions is higher than that inside the neighboring stiffer $M_{II,tilt}$ and matrix M_{II} regions. Therefore, the higher piezoresponse in the M_I regions can be attributed to the flexoelectric effect induced by the strain gradient. This result of higher piezoeresponse in M_I regions conflicts with the general understanding that the piezoelectricity of

Table I | FWHM of the X-ray diffraction peaks for the M_I and $M_{II,tilt}$ phases[a)]

		M_I	$M_{II,tilt}$
FWHM ($\times 10^{-3}$ r.l.u.)	Q_x	13.0	8.2
	Q_z	14.5	10.9

[a)]As the two diffraction peaks (left and right) of each phase are similar, only one FWHM is listed.

M_{II} phase is a higher than that of R phase[21]. It is because M_I phase is not a low energy state as other phases, and behaves differently from the ground R phase in piezoelectricity.

To estimate the strain magnitude in the mixed-phase M_I phase near the M_I and $M_{II,tilt}$ interface, a θ-2θ scan with respect to the surface normal of the M_I phase (Fig. 5a) is extracted from the RSM image (Fig. 3) at H = 0.041 r.l.u. It shows an asymmetric diffraction peak, indicating that the lattice constant c is not uniform in M_I phase. The peak is fitted by an asymmetric Gaussian function and the half widths at half maximum are $\sigma_h = 6.63\times10^{-3}$ r.l.u. on the high Q_z side and $\sigma_l = 7.89\times10^{-3}$ r.l.u. on the low Q_z side. σ_h presents the contributions of the normal distribution of lattice constant and the grain-size broadening. The larger σ_l indicates there is an additional component (σ_{sg}) due to strain gradient at phase boundaries. Assuming a combination of peak widths by $\sigma_l^2 = \sigma_h^2 + \sigma_{sg}^2$, σ_{sg} = 4.29×10^{-3} r.l.u. is obtained, corresponding to a strain of +0.47%. There is a strain in the compliant M_I phase at the boundary. To accommodate the lattice mismatch between M_I and $M_{II,tilt}$ phases (Fig. 5b), the more compliant M_I phase exhibits an expansion of the out-of-plane lattice constant by Δc_{M_I}, whereas Δc_{M_I} become its maximum at the interface. The strain relaxes with the distance apart from the phase boundary. Such a strain gradient supports the findings by UFM and PFM that the flexoeletric effect accounts for the extraordinary polarization in mixed-phase BFO thin films. The enhancement of polarization in the mixed-phase regions is about 55 μC/cm² from Ref. 22, the region with strain gradient is 17 nm in width (half width of M_I regions), and the volume fraction of the M_I phase is 50% according to topography. Therefore the flexoelectric coefficient of the M_I phase is estimated to be ≈ 1.4 μC/m by Eq. (1), which is comparable to that of perovskite ceramics in paraelectric phases[13].

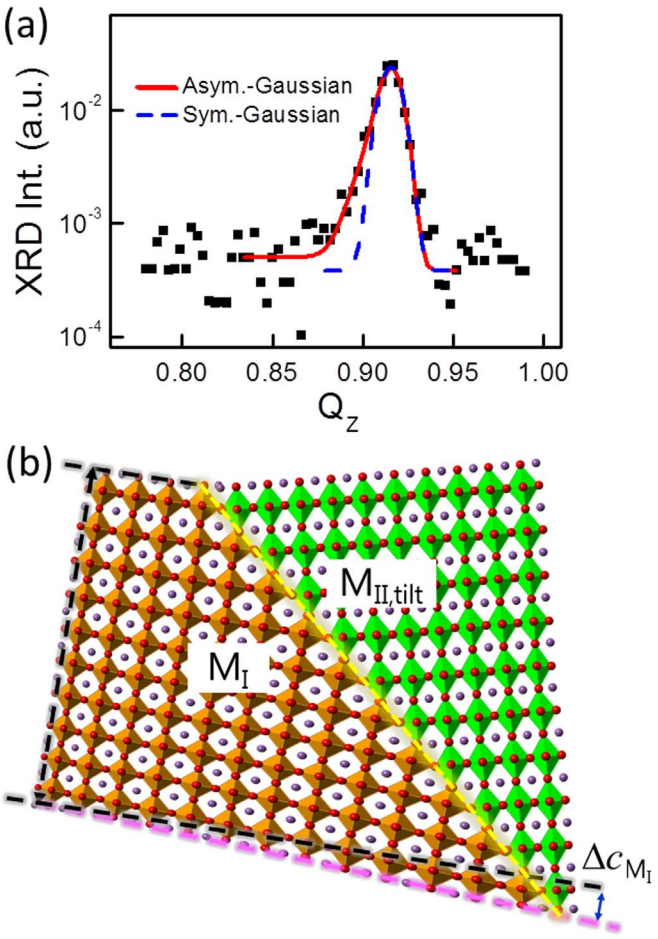

Figure 5 | (a) Asymmetric θ-2θ diffraction peak to the surface normal of the M_I phase extracted from the RSM image (Fig. 3) at H = 0.041 r.l.u. The peak can be better fitted by an asymmetric Gaussian function (red), while a symmetric Gaussian function (blue) is reported only to visualize the asymmetry of the peak. (b) Schematic illustration of the strain gradient of the M_I phase near the interface (yellow line) between the M_I (brown) and M_{II} (green) phases.

Discussion

The elastic response in the mixed-phased region of BFO thin films, epitaxially grown on LAO substrates, has been investigated by means of scanning probe microscopy and X-ray diffraction strain analysis. Ultrasonic force microscopy can spatially resolve the nanoscale elastic modulation and regions with low/high stiffness values topologically coincide with the $M_I/M_{II,tilt}$ phases. Although the M_I phase has a smaller unit-cell volume, it is more compliant than the other phases, as confirmed by X-ray diffraction strain analysis. Because of the flexoelectric effect, the elastic kink at the boundary produces the piezoresponse peak at the phase boundary and a higher elastic gradient on the M_I side produces a higher piezoresponse inside the M_I phase, resulting in an enhanced electromechanical response in the strained mixed-phase BFO films.

Methods

Mixed-phase BFO films are epitaxially grown on a single-crystal LAO substrate (LAO) by means of pulse laser deposition. The thickness of the samples herein reported is of around 70 nm. These BFO films are subjected to a highly compressive strain (> 4%), thus M_I and M_{II} phases coexist.

The AFM setup is made of a commercial probe head (NT-MDT, SMENA) with electronics and control software developed in-house. The cantilevers employed have a diamond-coated tip, a nominal spring constant of around 5.5 N/m and a resonant frequency of around 150 kHz (NT-MDT, DCP-01). To conduct UFM, the samples are mounted on a piezo-disc that can be driven at around 4 MHz with an amplitude modulation frequency of 3.7 kHz (Agilent 33220A) to generate a maximal oscillating amplitude below 1 nm. The piezoresponse of BFO films is characterized by PFM. PFM and UFM can be quickly switched from one to the other while the tip is still in contact. To collect the UFM and PFM data, a digital lock-in amplifier (Zurich, HF2LI) is employed. The color codes of the images are the following: brighter for higher regions in AFM, higher stiffness in UFM, and higher piezoelectricity in PFM. For UFM in particular, a brighter color represents a lower local indentation and thus corresponds to a stiffer region.

RSM has been performed using a standard Huber four-circle X-ray diffractometer operated at 50 kV and 200 mA with Cu $K_{\alpha1}$ radiation in the X-ray laboratory at National Synchrotron Radiation Research Center (NSRRC) in Hsinchu, Taiwan. The incident beam is monochromated with a flat Ge (111) crystal and two sets of slits serve to eliminate Cu $K_{\alpha2}$ so as to obtain a high wave-vector resolution of 0.01 nm^{-1} order in the reciprocal space. The reciprocal space map is recorded by a series of θ–2θ scans with different ω and plotted in the reciprocal lattice unit Q that is normalized to the LAO (001) substrate (1 r.l.u. = $2\pi/a_{LAO}$).

1. Zhang, J. X. *et al.* A nanoscale shape memory oxide. *Nat. Commun.* **4**, 3768 (2013).
2. Fu, H. X. & Cohen, R. E. Polarization rotation mechanism for ultrahigh electromechanical response in single-crystal piezoelectrics. *Nature* **403**, 281 (2000).

3. Chu, Y.-H. *et al.* Domain control in multiferroic $BiFeO_3$ through substrate vicinality. *Adv. Mater.* **19**, 2662 (2007).
4. Chu, Y.-H., Martin, L. W., Holcomb, M. B. & Ramesh, R. Controlling magnetism with multiferroics. *Mater. Today* **10**, 16 (2007).
5. Christen, H. M., Nam, J. H., Kim, H. S., Hatt, A. J. & Spaldin, N. A. Stress-induced R-M_A-M_C-T symmetry changes in $BiFeO_3$ films. *Phys. Rev. B* **83**, 144107 (2011).
6. Yang, J. C. *et al.* Orthorhombic $BiFeO_3$, *Phys. Rev. Lett.* **109**, 247606 (2012).
7. Zeches, R. J. *et al.* A strain-driven morphotropic phase boundary in $BiFeO_3$. *Science* **326**, 977 (2009).
8. Liu, H.-J. *et al.* Strain-driven phase boundaries in $BiFeO_3$ thin films studied by atomic force microscopy and x-ray diffraction. *Phys. Rev. B* **85**, 014104 (2012).
9. Zhang, J. X. *et al.* Large field-induced strains in a lead-free piezoelectric material. *Nat. Nanotechnol.* **6**, 98 (2011).
10. Damodaran, A. R. *et al.* Nanoscale structure and mechanism for enhanced electromechanical response of highly strained $BiFeO_3$ thin films. *Adv. Mater.* **23**, 3170 (2011).
11. Zhang, J. X., Zeches, R. J., He, Q., Chu, Y.-H. & Ramesh, R. Nanoscale phase boundaries: a new twist to novel functionalities. *Nanoscale* **4**, 6196 (2012).
12. He, Q. *et al.* Electrically controllable spontaneous magnetism in nanoscale mixed phase multiferroics. *Nat. Commun.* **2**, 225 (2011).
13. Zubko, P., Catalan, G. & Tagantsev, A. K. Flexoelectric effect in solids. *Annu. Rev. Mater. Res.* **43**, 387 (2013).
14. Kolosov, O. & Yamanaka, K. Nonlinear detection of ultrasonic vibrations in an atomic force microscope. *Jpn. J. Appl. Phys.* **32**, L1095 (1993).
15. Kolosov, O., Castell, M. R., Marsh, C. D. & Briggs, G. A. D. Imaging the elastic nanostructure of Ge islands by ultrasonic force microscopy. *Phys. Rev. Lett.* **81**, 1046 (1998).
16. Dinelli, F. *et al.* Mapping surface elastic properties of stiff and compliant materials on the nanoscale using ultrasonic force microscopy. *Phil. Mag. A*, **80**, 2299 (2000).
17. Chen, Y.-C. *et al.* Electrical control of multiferroic orderings in mixed-phase $BiFeO_3$ films. *Adv. Mater.* **24**, 3070 (2012).
18. Doig, K. I. *et al.* Coherent magnon and acoustic phonon dynamics in tetragonal and rare-earth-doped $BiFeO_3$ multiferroic thin films. *Phys. Rev. B* **88**, 094425 (2013).
19. Shang, S. L., Sheng, G., Wang, Y., Chen, L. Q. & Liu, Z. K. Elastic properties of cubic and rhombohedral $BiFeO_3$ from first-principles calculations. *Phys. Rev. B* **80**, 052102 (2009).
20. Dong, H., Chen, C., Wang, S., Duan, W. & Li, J. Elastic properties of tetragonal $BiFeO_3$ from first-principles calculations. *Appl. Phys. Lett.* **102**, 182905 (2013).
21. Ederer, C. & Spaldin, N. A. Effect of epitaxial strain on the spontaneous polarization of thin film ferroelectrics. *Phys. Rev. Lett.* **95**, 257601 (2005).
22. Zhang, J. X. *et. al.* Microscopic origin of the giant ferroelectric polarization in tetragonal-like $BiFeO_3$. *Phys. Rev. Lett.* **107**, 147602 (2011).

Acknowledgments

This work is supported by Ministry of Science and Technology of Taiwan (Grant NO. MOST 102-2112-M-029-005-MY3), and National Chiao Tung University (2013 NCTU Short-term Research Program Scholarship). The authors would like to thank Dr. P. Pinque of NEST, Istituto Nanoscienze-CNR and Scuola Normale Superiore for his kindly support.

Author contributions

C.-E.C., H.-J.L. and F.D. performed the experiments. H.-J.L. and Y.-H.C. contributed material. F.S.-S.C., F.D., Y.-H.C., Y.-C.C. and C.-S.C. conceived and designed the experiments. F.S.-S.C., Y.-H.C. and F.D. co-wrote the paper.

Additional information

Competing financial interests: The authors declare no competing financial interests.

How to cite this article: Cheng, C.-E. *et al.* Revealing the flexoelectricity in the mixed-phase regions of epitaxial $BiFeO_3$ thin films. *Sci. Rep.* **5**, 8091; DOI:10.1038/srep08091 (2015).